

# Optical repumping of triplet- $P$ states enhances magneto-optical trapping of ytterbium atoms

Jun Woo Cho,<sup>1,2</sup> Han-gyeol Lee,<sup>1</sup> Sangkyung Lee,<sup>1</sup> Jaewook Ahn,<sup>1,\*</sup> Won-Kyu Lee,<sup>2</sup> Dai-Hyuk Yu,<sup>2</sup>  
Sun Kyung Lee,<sup>2</sup> and Chang Yong Park<sup>2,†</sup>

<sup>1</sup>*Department of Physics, KAIST, Daejeon 305-701, Korea*

<sup>2</sup>*Korea Research Institute of Science and Standards, Daejeon 305-340, Korea*

(Received 21 November 2011; published 5 March 2012)

Radiative decay from the excited  $^1P_1$  state to metastable  $^3P_2$  and  $^3P_0$  states is expected to limit the attainable trapped atomic population in a magneto-optic trap of ytterbium (Yb) atoms. In experiments we have carried out with optical repumping of  $^3P_{0,2}$  states to  $^3P_1$ , we observe an enhanced yield of trapped atoms in the excited  $^1P_1$  state. The individual decay rate to each metastable state is measured and the results show excellent agreement with the theoretical values.

DOI: [10.1103/PhysRevA.85.035401](https://doi.org/10.1103/PhysRevA.85.035401)

PACS number(s): 37.10.De, 42.50.Ct, 95.30.Ky, 32.10.-f

Ytterbium (Yb,  $Z = 70$ ) is a rare-earth element of versatile internal level structure, generally referred to as singlet-triplet atomic system, and its narrow intercombination transitions between singlet and triplet spin manifolds have opened the possibility of many fundamental studies and applications, including optical frequency standards [1–3], parity nonconservation tests [4], and ultracold collision and scattering characterizations [5–10]. The natural abundance in Yb isotopes, furthermore, allows the photo-induced cold molecular formation of bosonic and fermionic and composite dimers [11]. Recent studies have revealed the sympathetic cooling of  $^{176}\text{Yb}$  below the transition temperature and the far-off-resonance trapping of fermionic degenerate  $^{173}\text{Yb}$  as well as the realization of Bose-Einstein condensation of  $^{174}\text{Yb}$  and  $^{170}\text{Yb}$  atoms [12–14].

The energy level structure and the decay rates of  $^{174}\text{Yb}$  are shown in Fig. 1. The blue transition with a relatively broad linewidth allows the optical excitation from the  $(6s^2)^1S_0$  ground state to the  $(6s6p)^1P_1$  excited state to be used in both Zeeman slowing and magneto-optical trapping (MOT). The radiative decay from the  $^1P_1$  excited state to the  $^3P_{0,2}$  triplet states via the  $^3D_2$  and  $^3D_1$  states, however, causes the loss of the trapped atoms and, as a result, limits the number of trapped atoms.

In this Brief Report, we report an experimental demonstration of a  $^{174}\text{Yb}$  MOT with optical repumping of the metastable states. We use additional laser systems to control the shelving losses to  $^3P_0$  and  $^3P_2$ , [i.e., optical repumping of the metastable atoms to the  $(6s7s)^3S_1$  state] and the atoms in the metastable states continuously decay to the ground state. By doing so, atom trapping is only hindered by the collisional loss and, as a result, the number and lifetime of trapped Yb atoms are increased. It is shown, in a master equation calculation performed to verify the atom trapping dynamics, that the trapped-atom collisions against ballistic Yb flux from the Zeeman slower plays a crucial role in reducing the measurement uncertainty. We have measured the individual decay rate to each metastable state, by minimizing the measurement uncertainty coming from Yb-Yb and Yb-background gas collisional losses, and the measured results show excellent agreement with the theoretical values.

We shall first describe the experimental setup where the repumping lasers are used to enhance the excited atomic population in the MOT. Then the calculated population variations of each level are given after solving the master equations. We present the experimental measurement of the decay rate to individual metastable states and then draw some conclusions.

Figure 2 shows the schematic setup for the cooling and trapping of  $^{174}\text{Yb}$  atoms. A standard six-beam MOT was constructed with a diode laser system that was injection-locked to a wavelength of 398.9 nm for the  $^1S_0$ - $^1P_1$  transition [ $\lambda_L = 398.9$  nm,  $\Gamma_0 = 28$  MHz (FWHM)] [15]. The master laser was a home-made external cavity diode laser (ECDL), which is 15 MHz red-detuned from the  $^{174}\text{Yb}$   $^1P_1$ - $^1S_0$  fluorescence peak. Then the master laser seeded two slave lasers respectively used for the trapping and Zeeman slowing.

For the Zeeman slower laser, a double-pass acousto-optic modulator was used to further red-detune the frequency by 500 MHz from the master laser frequency. The output power of the Zeeman slower laser was 20 mW. The effusive atomic  $^{174}\text{Yb}$  beam was generated from an oven heated at a temperature of 400 °C, while the oven nozzle was differentially heated at a higher temperature of 415 °C. The coil for the Zeeman slower was made of a 1-mm-diameter copper wire and was wound on a steplike 30-cm-long stainless-steel pipe with a 16-mm inner diameter. When the Zeeman slower laser was operated at the saturation laser intensity, the capture velocity was 260 m/s in the Zeeman slower with a peak magnetic field of 300 G. In the trap region the axial magnetic field gradient was  $dB/dz = 30$  G/cm, made by anti-Helmholtz coils. The Zeeman slower region was designed to maintain a nearly constant deceleration of 80 km/s<sup>2</sup> and the atomic beam flux was  $10^{10}$ – $10^{11}$  s<sup>-1</sup>.

The output power of the trap laser was up to 40 mW and, with this laser power, the fraction of the number of atoms in the excited state,  $f$ , was varied from 0.04 to 0.15. Here  $f$  is defined as

$$f = \frac{I/2I_s}{[1 + I/I_s + (2\Delta/\Gamma_0)^2]}, \quad (1)$$

where  $I$  is the laser intensity and the saturation intensity is  $I_s = 59$  mW/cm<sup>2</sup> for the  $^1S_0$ - $^1P_1$  transition. The number of atoms in the trap is typically  $N_o = 10^7$ , measured by a photomultiplier tube in the linear calibration region. The atom

\*jwahn@kaist.ac.kr

†cypark@kriss.re.kr

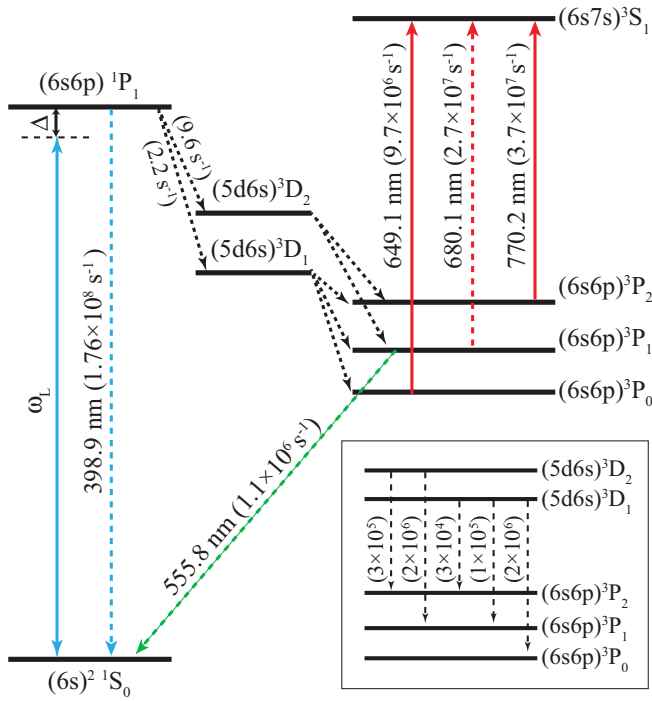


FIG. 1. (Color online) Simplified energy level diagram for  $^{174}\text{Yb}$  showing the main cooling transition at 398.9 nm, radiative channels for the  $^1P_1$  excited state, and the relevant repumping scheme (649.1 and 770.2 nm).  $\omega_L$  and  $\Delta$  are the  $^1S_0$ - $^1P_1$  cooling laser frequency and detuning, respectively. Numbers in parentheses give the transition Einstein A coefficients.

density, roughly calculated by  $N_o/V$ , where  $V = (\sqrt{\pi}a)^3$  is estimated from a Gaussian sphere,  $\exp(-r^2/a^2)$  with  $a = 2$  mm, is  $2 \times 10^5 \text{ mm}^{-3}$  (without repumping; this is the initial maximal density).

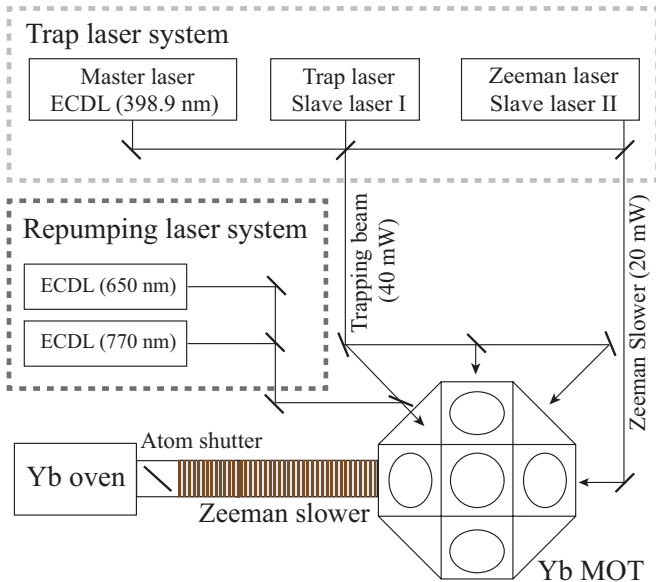


FIG. 2. (Color online) Schematic representation of the setup for the magneto-optical trapping of  $^{174}\text{Yb}$  atoms with repumping laser systems for  $^3P_2$ - $^3S_1$  and  $^3P_0$ - $^3S_1$  transitions. ECDL is an acronym for external cavity diode laser.

To investigate the enhancement of the trapped atom yield by controlling the shelving loss to the triplet states, the  $^3P_0$  and  $^3P_2$  states were repumped to  $^3S_1$  by additional lasers. We used two repumping laser systems (ECDL) at wavelengths of 649.1 and 770.2 nm, respectively, frequency-locked to  $^3P_0$ - $^3S_1$  and  $^3P_2$ - $^3S_1$  transition fluorescence signals. For laser frequency calibration, two more laser systems (ECDL) at wavelengths of 556 and 680 nm were used to induce two-photon transitions  $^1S_0$ - $^3P_1$ - $^3S_1$  and the fluorescence signal was modulation-locked to the  $^3P_2$ - $^3S_1$  and  $^3P_0$ - $^3S_1$  transitions.

By considering the slow decays from the  $^1P_1$  state to the  $^3D_{1,2}$  compared with ones from the  $^3D_{1,2}$  to the  $^3P_{0,1,2}$ , in the time scale of the cooling and trapping process, an equivalent system for the  $^{174}\text{Yb}$  atom is a five-level system. For the states denoted by  $|g\rangle = ^1S_0$ ,  $|e\rangle = ^1P_1$ ,  $|0\rangle = ^3P_0$ ,  $|1\rangle = ^3P_1$ , and  $|2\rangle = ^3P_2$ , the rate equations are given as

$$\frac{d}{dt}(N_g + N_e) = \eta - (a_0 + a_1 + a_2)N_e + \gamma_1 N_1 - \gamma_c(N_g + N_e), \quad (2)$$

$$\frac{dN_0}{dt} = a_0 N_e - \gamma_c N_0, \quad (3)$$

$$\frac{dN_1}{dt} = a_1 N_e - \gamma_c N_1 - \gamma_1 N_1, \quad (4)$$

$$\frac{dN_2}{dt} = a_2 N_e - \gamma_c N_2, \quad (5)$$

where  $\eta$  is the loading rate of the MOT,  $a_{i(i=0,1,2)}$  are the decay rates from the excited state to the  $^3P_i$  states,  $\gamma_c$  is the background collisional loss rate, and  $\gamma_1$  is the spontaneous decay rate of  $^3P_1$  to the ground state. Including the Yb-Yb collisional term, which is not negligible for some cases in our experiment, the equation for the number of trapped atoms,  $N = N_g + N_e$ , becomes

$$\frac{dN}{dt} = \eta - [a_{2,0}f(P_T, \Delta) + \gamma_c(f)]N - \beta(f)N^2, \quad (6)$$

where  $a_{2,0}$  is the decay rate of  $^1P_1$  atoms to both metastable  $^3P_{0,2}$  states,  $P_T$  is the total trap laser power, and  $\beta(f)$  is the Yb-Yb collision coefficient [16].

In theory, the decay rates are given as  $a_0 = 6.18 \text{ s}^{-1}$ ,  $a_1 = 5.25$ , and  $a_2 = 0.37$  [17]. When the atoms in either the  $^3P_0$  state or the  $^3P_2$  state are optically pumped to the  $^3S_1$  state, they spontaneously decay to the three  $^3P_{0,1,2}$  states with a branching ratio of  $\lambda_0:\lambda_1:\lambda_2 = 1:3:5$ , and the atoms in the  $^3P_1$  state immediately decay to the ground state. So, we can consider the following four different repumping cases: (NR) no repumping case, (A) repumping the  $^3P_2$  state only, (B) repumping the  $^3P_0$  state only, and (A + B) repumping both  $^3P_{0,2}$  states. In the NR case, the net decay rate of the trapped atom is given as  $a_{NR} = a_0 + a_2 = 6.55 \text{ s}^{-1}$ , simply from Eqs. (3) and (5). In case A, however, the atoms in the  $^3P_2$  state are distributed to the  $^3P_0$  and  $^3P_2$  states and  $a_0$  in Eq. (3) becomes  $a'_0 = a_0 + \frac{\lambda_1}{\lambda_1 + \lambda_0} a_2 = 6.28$ , from the  $^1S_1$  state to the  $^3P_{0,1,2}$  states. So, the net decay rate of the trapped atoms for case A is  $a_A = 6.28 \text{ s}^{-1}$ . Likewise, in case B,  $a_2$  in Eq. (5) becomes  $a'_2 = a_2 + \frac{\lambda_2}{\lambda_2 + \lambda_1} a_0 = 3.94$  and, therefore, the decay rate for case B is obtained as  $a_B = 3.94 \text{ s}^{-1}$ . In case A + B, both  $^3P_{0,2}$  states are repumped, and the net decay rate to the triplet  $P$  states become zero (i.e.,  $a_{A+B} = 0$ ).

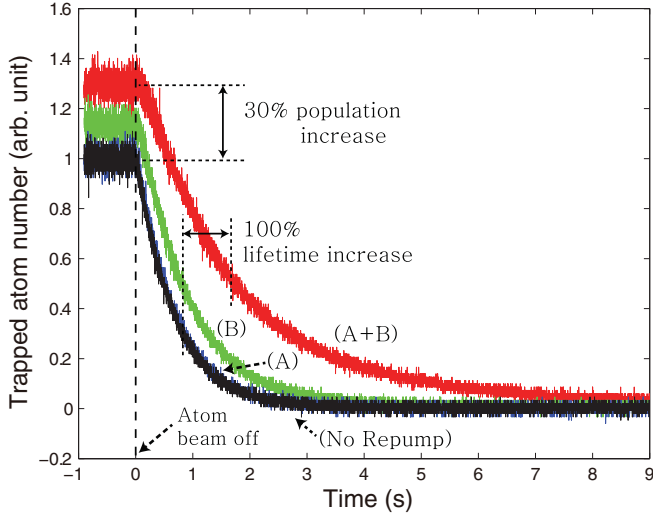


FIG. 3. (Color online) The decay dynamics of  $^{174}\text{Yb}$  MOT for the three different repumping cases: (A) repumping the  $^3P_2$  state, (B) repumping the  $^3P_0$ , and (A + B) repumping both states. The trapped atom numbers are estimated with the fluorescence from the trapped atoms in the  $^1P_1$  state. The experimental data for case (A) is almost overlaid with the (No Repump) case.

We investigate the decay dynamics of the trapped atoms in the MOT by shutting off the atomic beam and measuring the  $^1P_1\text{-}^1S_0$  fluorescence signal as a function of time. The experimental situation for zero Yb flux is the condition  $\eta = 0$  in Eq. (6), and its solution is given by Ref. [18]

$$N(t) = N(0)e^{-\Gamma t} \left[ 1 + \frac{\beta N(0)}{\Gamma} (1 - e^{-\Gamma t}) \right]^{-1}, \quad (7)$$

where  $\Gamma$  is the loss rate of the MOT defined similarly as the square bracket in Eq. (6) as

$$\Gamma = a_x f(P_T, \Delta) + \gamma_c(f), \quad (8)$$

and the index  $x$  in  $a_x$  indicates a particular experiment among the four repumping cases (i.e.,  $x \in \{(NR), (A), (B), (A + B)\}$ ). Figure 3 shows typical behavior of the temporal evolution of the number of trapped atoms,  $N(t)$ , in the MOT, for all four repumping cases. Both the lifetime  $\tau$  of the MOT, which is measured as the  $1/e$  decay time, and the steady-state trapped atom number  $N(0)$  are increased by the repumping of the metastable states. The figure shows that, when the repumping scheme (A + B) has increased  $\tau$  by 100%,  $N(0)$  has increased by only 30%. This result is not consistent with the fact that the change of  $N(0)$  should be proportional to the change of  $\tau$ , or  $N(0) = \eta\tau$ , as  $\tau = 1/\Gamma$  and  $N_0 = \eta/\Gamma$  from Eqs. (6) and (8). However, the collisional loss term  $\gamma_c$  in Eq. (8) is, in fact, factored into two parts: one due to the background residual gas in the chamber and the other due to the Yb flux from the Zeeman slower. Therefore, the collisional loss term is a function of the loading rate  $\eta$ , i.e.,  $\Gamma = \Gamma(\eta)$ , and, as a result, shutting off the atomic beam has suddenly reduced the loss rate  $\Gamma$ . It is noted that the last term in Eq. (6) is responsible for the collision between cold Yb atoms captured in the MOT, not the collision between the Yb in the MOT and the Yb in the atomic beam from the Zeeman slower.

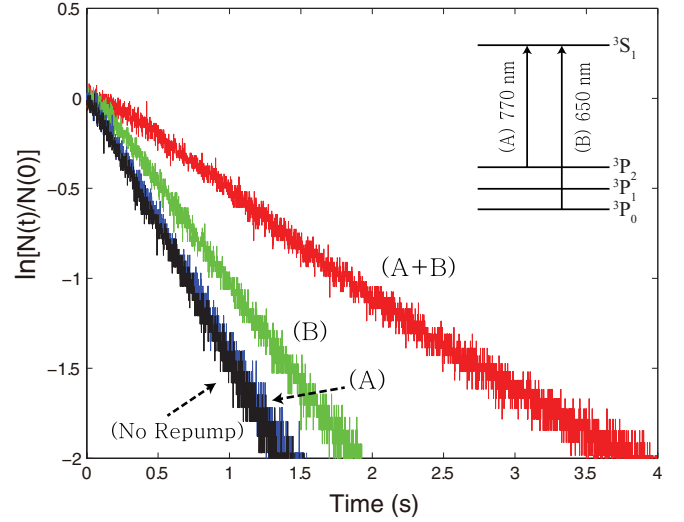


FIG. 4. (Color online) Measurement of the temporal evolution of the trapped atom number of the  $^{174}\text{Yb}$  MOT. The result is induced from the  $^1P_1\text{-}^1S_0$  fluorescence signal obtained for the four different repumping cases: (NR) no repumping, (A) repumping the  $^3P_2$  state only, (B) repumping the  $^3P_0$  state only, and (A + B) repumping both states. The inset shows the corresponding  $^{174}\text{Yb}$  energy levels.

Figure 4 shows the measured results on a logarithmic scale, where  $N(t)$ , scaled with  $N(0)$ , is plotted as a function of time. The experiments were performed for values of  $\beta N(0)/\Gamma$  varying from 0 to 1 so that the second term in the parentheses in Eq. (7) needs to be included in a fitting of  $\Gamma$ . It is also noted that the low-density condition for the trapped atomic distribution is still fulfilled [5,18,19]. This is especially clear from the behavior of the (A + B) data, shown in red in Fig. 4, which deviates significantly from a linear line in the given logarithmic plot.

In order to measure  $\Gamma$  for the four different repumping cases, we have performed an experiment for the temporal

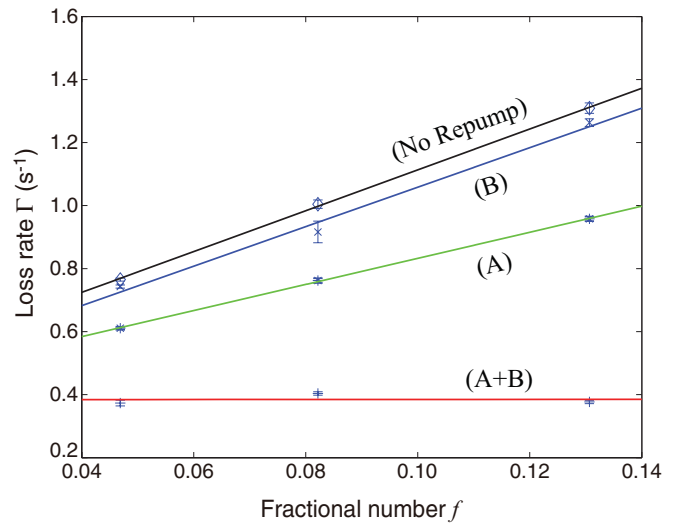


FIG. 5. (Color online) Measured loss rate ( $\Gamma$ ) vs the number of atoms in the excited state ( $f$ ), obtained for the four different repumping cases. The slopes ( $\Delta\Gamma/\Delta f$ ) were measured as 6.48, 6.27, 4.14, and less than  $6.3 \times 10^{-3}$ , from the top to the bottom curves.

TABLE I. Summary of the measured decay rates  $a_0$  and  $a_2$  of  $^{174}\text{Yb}$  atoms. Numbers are all in inverse seconds.

	This work	Previous works [16,20]	Theory [17]
$a_{2,0}$	6.48 (2.11)	23 (11)	6.6
$a_0$	5.96 (1.97)		6.18
$a_2$	0.42 (0.14)		0.37
$a_1$		21.3 (2.6)	5.2

evolution of the  $^1P_1$ - $^1S_0$  fluorescence at three different trap laser power conditions. The data have been numerically fitted to Eq. (7) to obtain  $\Gamma(f)$ , and the results are shown in Fig. 5. The graphs show the linear dependence of  $\Gamma$  on  $f$  for all four repumping cases. A linear regression analysis predicts that all four lines can be extrapolated to converge at  $0.42 \pm 0.03$  as  $f$  approaches zero. It is also predicted that the slopes of the fitted lines, that is, the decay rate  $a_x$  in Eq. (7), turns out to be  $a_{\text{NR}} = 6.48$ ,  $a_{\text{A}} = 6.27$ ,  $a_{\text{B}} = 4.14$ , and  $a_{\text{A+B}} \leq 6.3 \times 10^{-3}$ . It is noted that the slope for the (A + B) case suggests that the background collision rate of the trapped atom depends little on  $f$ .

Using the obtained loss rates, we can estimate the decay rates  $a_0$ ,  $a_2$ , and  $a_{0,2}$ , etc, and the results are summarized in Table I. Despite the measurement uncertainty, the newly measured values for the individual decay rates  $a_0$  and  $a_2$  show good agreement with the theoretically predicted values, and the measurement accuracy is significantly improved, compared to

the previous experiments carried out by Loftus *et al.* [16]. The main uncertainty comes from the estimation of  $f$ , as the uncertainty of the saturation parameter  $s$  is caused by the power fluctuation, the spatial beam profile, and the measurement error of the trap laser power. Also, the uncertainty of  $\Delta/\Gamma$  is caused by the magnetic field in the trap, laser frequency detuning, etc., and its uncertainty is estimated to be 30%. Including the uncertainty in error fitting, the resulting uncertainty of the decay rate is estimated to be 33%. As shown in Table I, within the range of uncertainty, our measurement agrees well with the theoretically predicted results.

We have investigated the trapping dynamics of the  $^{174}\text{Yb}$  MOT by eliminating the shelving loss to the metastable  $^3P_{0,2}$  states via optical repumping. At the zero Yb loading limit, the individual decay rate to each metastable state is accurately measured, showing excellent agreement with the result of master equation calculation. With the use of optical repumping, a faster and a more efficient operation of Yb trapping has become possible, and it is hoped that this result may contribute to Bose-Einstein condensate research as well as to uncertainty evaluations with optical lattice clocks.

This research was supported by the Basic Science Research and Mid-career Researcher Programs through the National Research Foundation of Korea (NRF) funded by the Ministry of Education, Science and Technology (2009-0090843 and 2010-0013899).

- 
- [1] N. Poli, Z. W. Barber, N. D. Lemke, C. W. Oates, L. S. Ma, J. E. Stalnaker, T. M. Fortier, S. A. Diddams, L. Hollberg, J. C. Bergquist, A. Brusch, S. Jefferts, T. Heavner, and T. Parker, *Phys. Rev. A* **77**, 050501(R) (2008).
- [2] T. Kohno, M. Yasuda, K. Hosaka, H. Inaba, Y. Nakajima, and F.-L. Hong, *Appl. Phys. Express* **2**, 072501 (2009).
- [3] N. D. Lemke, A. D. Ludlow, Z. W. Barber, T. M. Fortier, S. A. Diddams, Y. Jiang, S. R. Jefferts, T. P. Heavner, T. E. Parker, and C. W. Oates, *Phys. Rev. Lett.* **103**, 063001 (2009).
- [4] D. DeMille, *Phys. Rev. Lett.* **74**, 4165 (1995).
- [5] J. Weiner, V. Bagnato, S. Zilio, and P. S. Julienne, *Rev. Mod. Phys.* **71**, 1 (1999).
- [6] T. P. Dinneen, K. R. Vogel, E. Arimondo, J. L. Hall, and A. Gallagher, *Phys. Rev. A* **59**, 1216 (1999).
- [7] G. Zinner, T. Binnewies, F. Riehle, and E. Tiemann, *Phys. Rev. Lett.* **85**, 2292 (2000).
- [8] R. Ciurylo, E. Tiesinga, S. Kotochigova, and P. S. Julienne, *Phys. Rev. A* **70**, 062710 (2004).
- [9] V. A. Dzuba, V. V. Flambaum, and J. S. M. Ginges, *Phys. Rev. A* **76**, 034501 (2007).
- [10] M. Machholm, P. S. Julienne, and K. A. Suominen, *Phys. Rev. A* **64**, 033425 (2001).
- [11] M. Kitagawa, K. Enomoto, K. Kasa, Y. Takahashi, R. Ciurylo, P. Naidon, and P. S. Julienne, *Phys. Rev. A* **77**, 012719 (2008).
- [12] Y. Takasu, K. Maki, K. Komori, T. Takano, K. Honda, M. Kumakura, T. Yabuzaki, and Y. Takahashi, *Phys. Rev. Lett.* **91**, 040404 (2003).
- [13] T. Fukuhara, Y. Takasu, M. Kumakura, and Y. Takahashi, *Phys. Rev. Lett.* **98**, 030401 (2007).
- [14] T. Fukuhara, S. Sugawa, M. Sugimoto, S. Taie, and Y. Takahashi, *Phys. Rev. A* **79**, 041604 (2009).
- [15] C. Y. Park and T. H. Yoon, *Phys. Rev. A* **68**, 055401 (2003).
- [16] T. Loftus, J. R. Bochinski, R. Shivitz, and T. W. Mossberg, *Phys. Rev. A* **61**, 051401(R) (2000).
- [17] S. G. Porsev, Y. G. Rakhlin, and M. G. Kozlov, *Phys. Rev. A* **60**, 2781 (1999).
- [18] M. Prentiss, A. Cable, J. E. Bjorkholm, S. Chu, E. L. Raab, and D. E. Pritchard, *Opt. Lett.* **13**, 452 (1988).
- [19] L. Marcassa, V. Bagnato, Y. Wang, C. Tsao, J. Weiner, O. Dulieu, Y. B. Band, and P. S. Julienne, *Phys. Rev. A* **47**, R4563 (1993).
- [20] K. Honda, Y. Takahashi, T. Kuwamoto, M. Fujimoto, K. Toyoda, K. Ishikawa, and T. Yabuzaki, *Phys. Rev. A* **59**, R934 (1999).